Electronic Supporting Information

Assembling Lanthanide–Transition Metal Clusters on TiO_2 for Photocatalytic Nitrogen Fixation

Chao-Long Chen,[1] Hai-Ying Wang,[1] Jun-Ping Li,[1] La-Sheng Long,[1,2] Xiang-Jian Kong,*[,1,2] and Lan-Sun Zheng[1,2]

[1] *Collaborative Innovation Center of Chemistry for Energy Materials, State Key Laboratory of Physical Chemistry of Solid Surfaces and Department of Chemistry, College of Chemistry and Chemical Engineering, Xiamen University, Xiamen, 361005, China.*

[2] *Innovation Laboratory for Sciences and Technologies of Energy Materials of Fujian Province (IKKEM), Xiamen, China*

1 Experimental Section

1.1 Chemicals

Titanium oxysulfate ($TiOSO_4$•$2H_2O$), Nickle nitrate hexahydrate ($Ni(NO_3)_2$•$6H_2O$), Iminodiacetic acid (H_2IDA), Europium chloride hexahydrate ($EuCl_3$•$6H_2O$), Gadolinium nitrate hexahydrate ($Gd(NO_3)_3$•$6H_2O$), Praseodymium nitrate hexahydrate ($Pr(NO_3)_3$•$6H_2O$), Neodymium nitrate hexahydrate ($Nd(NO_3)_3$•$6H_2O$), Sodium hydroxide (NaOH), Ethanol absolute (C_2H_5OH), Glycerol ($C_3H_8O_3$) Potassium hydroxide (KOH), Potassium Sodium Tartrate($NaKC_4H_4O_6$), Nessler's reagent (K_2HgI_4) are analytical grade, and used as received without further purification. Deionized water (18.6 MΩ) was made by the U.S.A ultrapure water meter (MILLIPORE).

1.2 Sample Preparation

1.2.1 Synthesis of clusters

1.2.1.1 Synthesis of $[Eu_{52}Ni_{56}(IDA)_{48}(OH)_{154}(H_2O)_{38}]$•$Cl_{12}(NO_3)_6$•$(H_2O)_{144}$

A mixture of $Ni(NO_3)_2$•$6H_2O$ (1.163 g, 4 mmol), $EuCl_3$•$6H_2O$ (0.902 g, 2.00 mmol), and H_2IDA (0.266 g, 2.00 mmol) were dissolved in deionized water (10.0 mL), then 1.0 mol/L NaOH aqueous solution was added dropwise in the above mixture until to the point of incipient but permanent precipitation. The mixture was heated to reflux for two hours and then filtered while hot. Block-shaped green crystals of **$Eu_{52}Ni_{56}$** were obtained in 50% yield (based on IDA) after the filtrate was kept at room temperature for 1 week. For $Eu_{52}Ni_{56}C_{192}O_{412}H_{490}N_{54}Cl_{12}$ (FW = 21762.45, based on 10 coordinated water): C, 10.6; H, 2.27; N, 3.48. Found: C, 10.28; H, 2.02; N, 3.57.

1.2.1.2 Synthesis of $[Pr_{52}Ni_{56}(IDA)_{48}(OH)_{154}(H_2O)_{38}]\bullet(NO_3)_{18}\bullet(H_2O)_{152}$

$Pr_{52}Ni_{56}$ was synthesized by the same method except the substitution of $EuCl_3\bullet 6H_2O$ to $Pr(NO_3)_3\bullet 6H_2O$. For $Pr_{52}Ni_{56}C_{192}O_{452}H_{502}N_{66}$ (FW = 21439.42, based on 20 coordinated water): C, 10.68; H, 2.34; N, 4.28. Found: C, 10.71; H, 2.05; N, 4.23.

1.2.1.3 Synthesis of $[Nd_{52}Ni_{56}(IDA)_{48}(OH)_{154}(H_2O)_{38}]\bullet(NO_3)_{18}\bullet(H_2O)_{152}$

$Nd_{52}Ni_{56}$ was synthesized by the same method except the substitution of $EuCl_3\bullet 6H_2O$ to $Nd(NO_3)_3\bullet 6H_2O$. For $Nd_{52}Ni_{56}C_{192}O_{472}H_{542}N_{66}$ (FW = 22115.83, based on 40 coordinated water): C, 10.43; H, 2.47; N, 4.18. Found: C, 10.44; H, 2.45; N, 4.16.

1.2.1.4 Synthesis of $[Gd_{52}Ni_{56}(IDA)_{48}(OH)_{154}(H_2O)_{38}]\bullet(NO_3)_{18}\bullet(H_2O)_{150}$

$Gd_{52}Ni_{56}$ was synthesized by the same method except the substitution of $EuCl_3\bullet 6H_2O$ to $Gd(NO_3)_3\bullet 6H_2O$. For $Gd_{52}Ni_{56}C_{192}O_{525}H_{644}N_{66}$ (FW = 23743.13, based on 85 coordinated water): C, 9.71; H, 2.73; N, 3.89. Found: C, 9.86; H, 2.74; N, 3.86.

For more information on the structure and analysis of crystals, refer to our reported literature.[1]

1.2.2 Synthesis of Titanium dioxide (TiO_2)

TiO_2 adopted a simple one-step hydrothermal synthesis method. In a special PTFE high-pressure reactor, 0.16 g $TiOSO_4\bullet 2H_2O$, 5 mL absolute alcohol, 3 mL deionized water, 2 mL glycerol are mixed well under magnetic stirring for 2 h. The mixture was then moved into oven and kept at 160 °C for 10 h, followed by natural cooling to room temperature. Finally, the precipitate was washed thoroughly with deionized water and alcohol, dried at 60 °C in drying cabinet for overnight.

1.2.3 Synthesis of Lanthanide–Transition Metal Clusters modified TiO_2

Based on the synthesis of TiO_2, different volume of 1 mmol/L $Eu_{52}Ni_{56}$ aqueous solution (0.1, 0.2, 0.5, 0.7, and 1 mL) were added to mixed solution with magnetic stirring for 2 h, then the mixed suspension moved into oven and kept at 160 °C for 10 h, followed by natural cooling to room temperature. Finally, the precipitate was washed thoroughly with deionized water and alcohol, dried at 60 ^oC in drying cabinet for overnight. The resulting samples were marked as $Eu_{52}Ni_{56}/TiO_2$-1, $Eu_{52}Ni_{56}/TiO_2$-2, $Eu_{52}Ni_{56}/TiO_2$-3, $Eu_{52}Ni_{56}/TiO_2$-4, and $Eu_{52}Ni_{56}/TiO_2$-5, respectively. Similarly, replacing $Eu_{52}Ni_{56}$ with $Pr_{52}Ni_{56}/Nd_{52}Ni_{56}/Gd_{52}Ni_{56}$ (the optimal amount: 0.5 mL), got the compounds $Pr_{52}Ni_{56}/TiO_2$-3, $Nd_{52}Ni_{56}/TiO_2$-3, and $Gd_{52}Ni_{56}/TiO_2$-3.

2 Characterization

The powder X-ray diffraction (XRD) images were recorded on Rigaku Ultima-IV instrument using Cu Kα radiation at 40 kV and 30 mA. Scanning electron microscopy (SEM) images were taken with a ZEISS Sigma scanning electron microscope. Transmission electron microscopy (TEM), High-resolution TEM (HRTEM), and high-angle annular dark-field scanning TEM (HAADF-STEM) were acquired on JEM-2100 and FEI TALOS F200. UV-visible diffused reflectance spectra (UV-DRS) were observed using a Cary 5000 UV-Vis spectrometer (Viarian, U.S.A). The photoluminescence spectra were recorded on a Molecular Fluorescence Spectrometer (F7000). Time-resolved PL decay curves were analysed with a FLS980 fluorescence lifetime spectrophotometer (Edinburgh Instruments, UK) under the excitation at 450 nm. UV spectrum were tested by Shimadzu UV-2550. The X-ray photoelectron spectroscopy (XPS) spectra were obtained on an ESCALAB Xi+. Electron paramagnetic resonance (EPR) spectra were displayed with Bruker EMX-10/12 electron paramagnetic resonance spectrometer at 110K and 293K. Ion chromatography (IC) data were collected using Metrohm 930 instrument, the cation mode adopted Metrosep C 5-150 as the column and 4mM HNO_3 as the eluent.

3 Photoelectrochemical measurements

All related tests involving electrochemistry were tested on the Shanghai Chenhua electrochemical workstation. In a standard three-electrode system, Ag/AgCl was used as the reference electrode, platinum wire was used as the counter electrode, and the catalyst-supported FTO glass was used as the working electrode. In detail, the prepare materials of working electrode including 5mg catalysts, 650 μL deionized water, 250 μL isopropanol, and 100 μL naphthol. The above-mentioned mixed slurry was evenly smeared on FTO glass with a range of 1×1 cm after ultrasonic. Electrochemical Impedance Spectroscopy (EIS) measurements recorded over a frequency range of 100 kHz-1000 kHz with ac amplitude of 20 mV at 0V. Photocurrent was tested in I-t mode, the light source is a 300W xenon lamp. The Mott-Schottky plots adopted an alternating current (AC, 1000 Hz, 1200 Hz and 1500 Hz). All the tests described above were used 0.2 M Na_2SO_4 (pH = 5.7) aqueous solution as the electrolyte. The potentials reported in this work were converted to reversible hydrogen electrode (RHE) scale via calibration with the following equation: E (vs. RHE) = E (vs. Ag/AgCl) + 0.059 × pH + 0.197 V.

4 Photocatalytic nitrogen reduction reaction measurements

In a double-jacketed quartz reactor, water was used to cool the reaction at room temperature. The light source is a high-pressure xenon lamp (λ>300 nm) produced by CEAU Light Company (Beijing, China), the light intensity was about 350 $mW\cdot cm^{-2}$. Specifically, 10mg of the photocatalysts was dispersed evenly in 30 mL ultrapure water in the quartz container with magnetic stirring. Placed the whole device in the dark and bubbled with high purity nitrogen (99.999%) at a rate of 60 mL/min for 30 min. The nitrogen was passed through a wash bottle containing 0.01 M sulfuric acid solution prior to use to remove possible interferents. As the reaction progresses, 2 mL reaction solution was extracted every 15 minutes intervals. After the reaction is over, the NH_4^+ concentration was calculated by the Nessler reagent method at 420 nm with the Shimadzu UV-2550 spectrometer after filtered the reaction liquid with a membrane.

5 Ammonia detection

The content of ammonia were detected by the Nessler reagent colorimetric method,[2] which were monitored by Shimadzu UV-2550 spectrometer at 420 nm. In front of the monitor, 500 g/L $NaKC_4H_4O_6$ solution was configured as a masking agent, which is keep boiling for 30 minutes to remove as much ammonia as possible. Additionally, Nessler's reagent as a developer was configured, 7.0125 g KOH, 3.6392 g K_2HgI_4 dissolved in 100 mL ultrapure water and ultrasound to obtain a clear mixed solution. 2 mL reaction solution added 0.5 mL masking agent and 0.5mL developer, measured at 420 nm with the Shimadzu UV-2550 spectrometer after 10 minutes of reaction. Ion chromatography (IC) was also used to verify the accuracy of the yield.

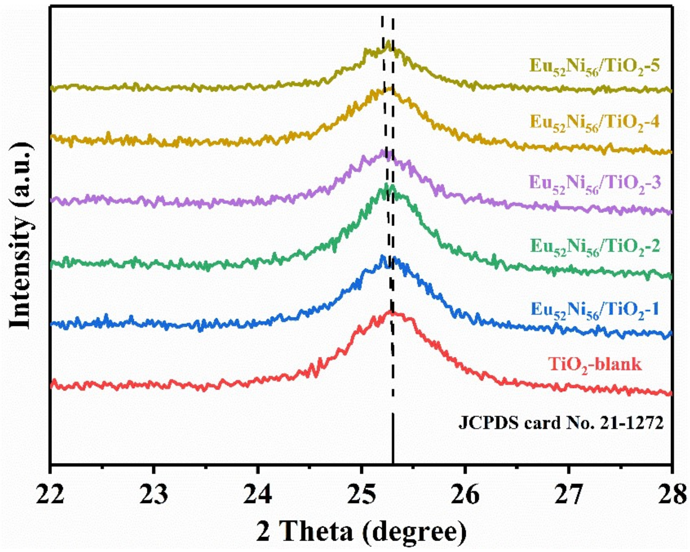

Figure S1. Small range PXRD profile of TiO_2-blank and $Eu_{52}Ni_{56}/TiO_2$-1, 2, 3, 4, 5.

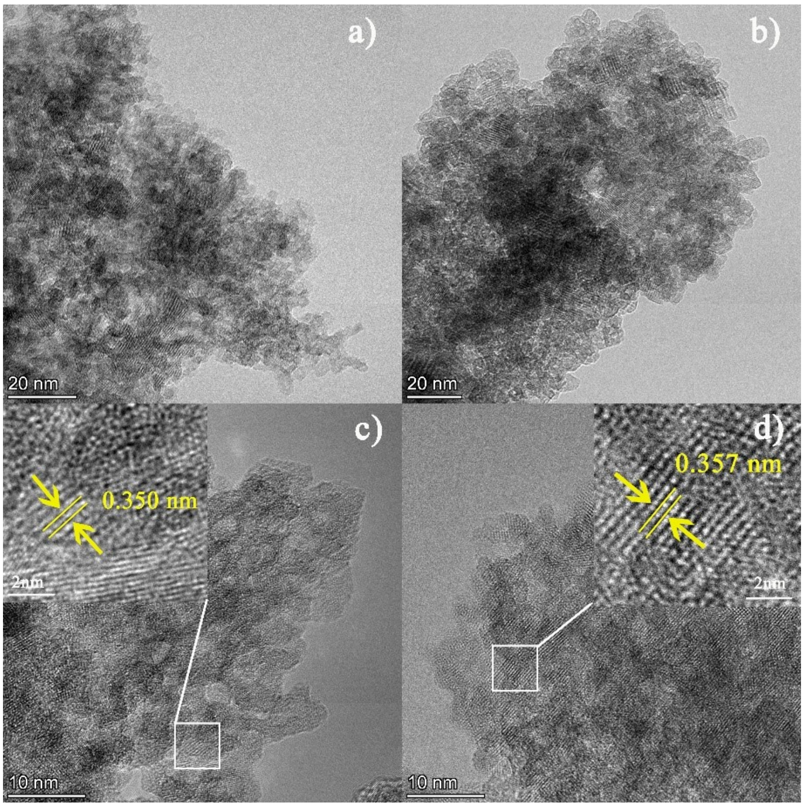

Figure S2. TEM profiles of (a) TiO_2-blank. (b) $Eu_{52}Ni_{56}/TiO_2$-3. (c) The lattice spacing of TiO_2-blank. (d) The lattice spacing of $Eu_{52}Ni_{56}/TiO_2$-3.

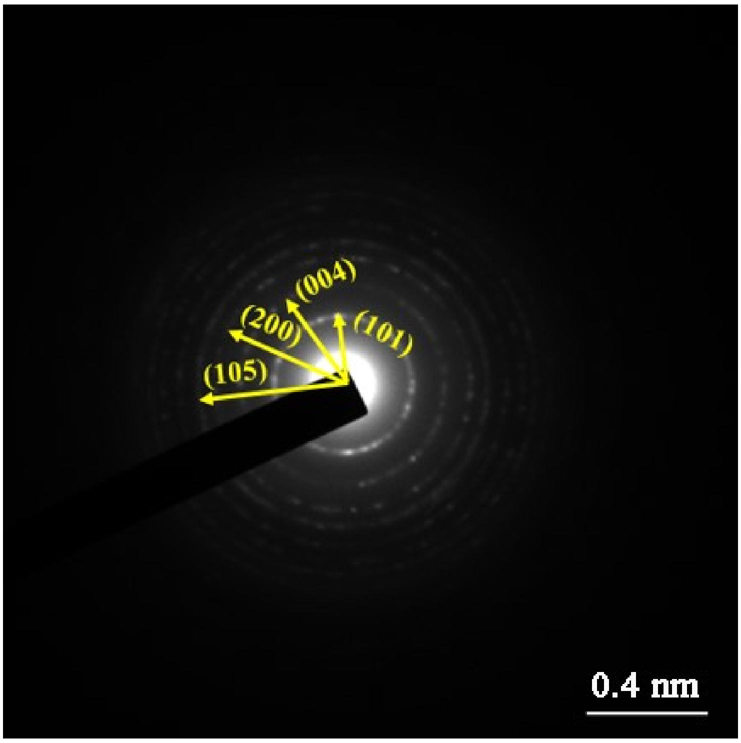

Figure S3. SAED profile of $Eu_{52}Ni_{56}/TiO_2$-3.

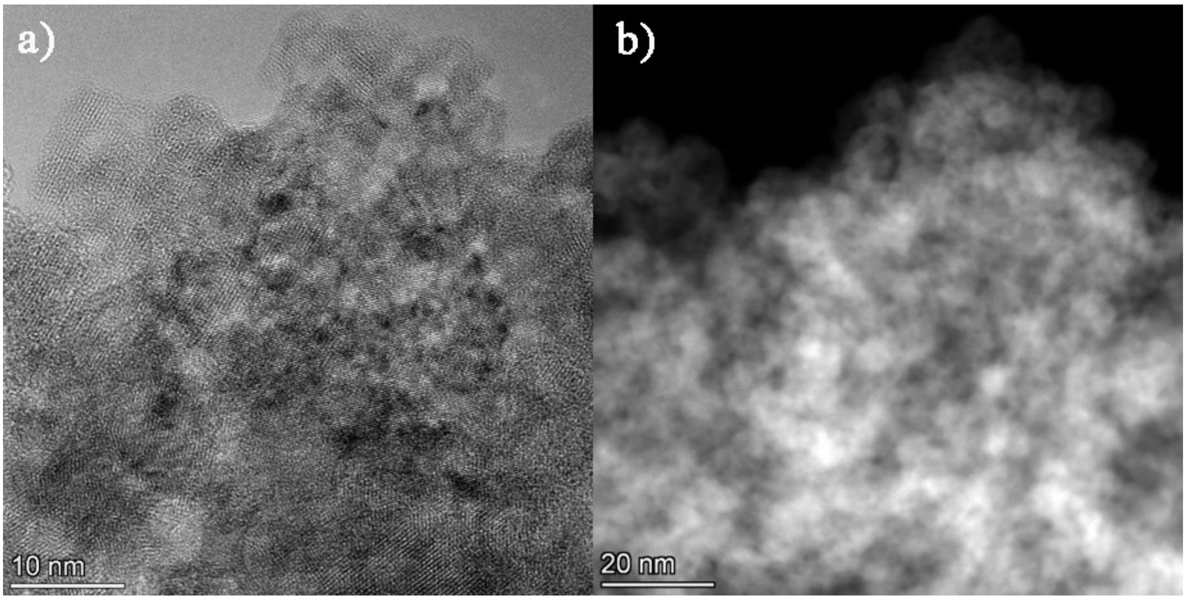

Figure S4. HRTEM and HAADF-STEM profiles of $Eu_{52}Ni_{56}/TiO_2$-3.

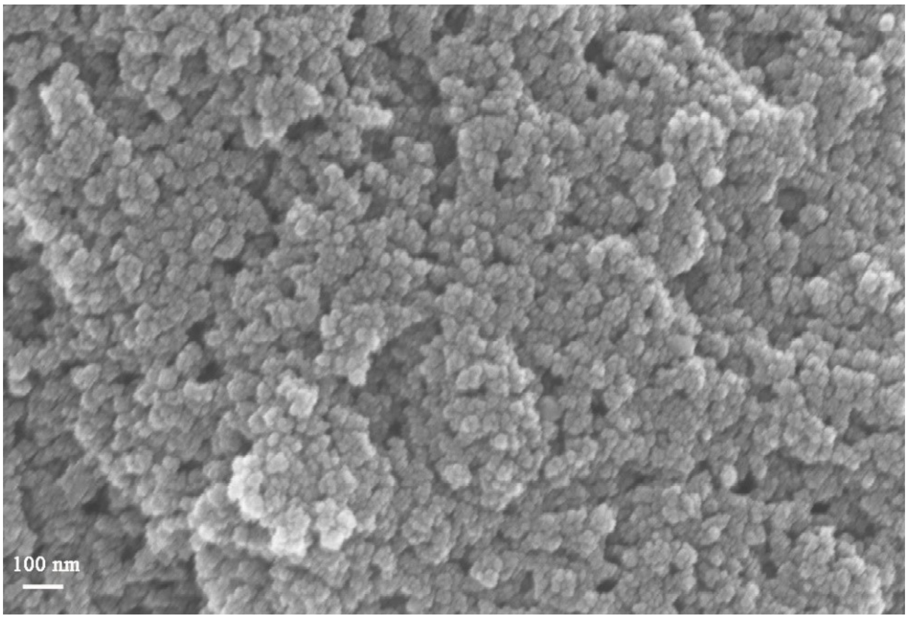

Figure S5. SEM profile of TiO_2-blank.

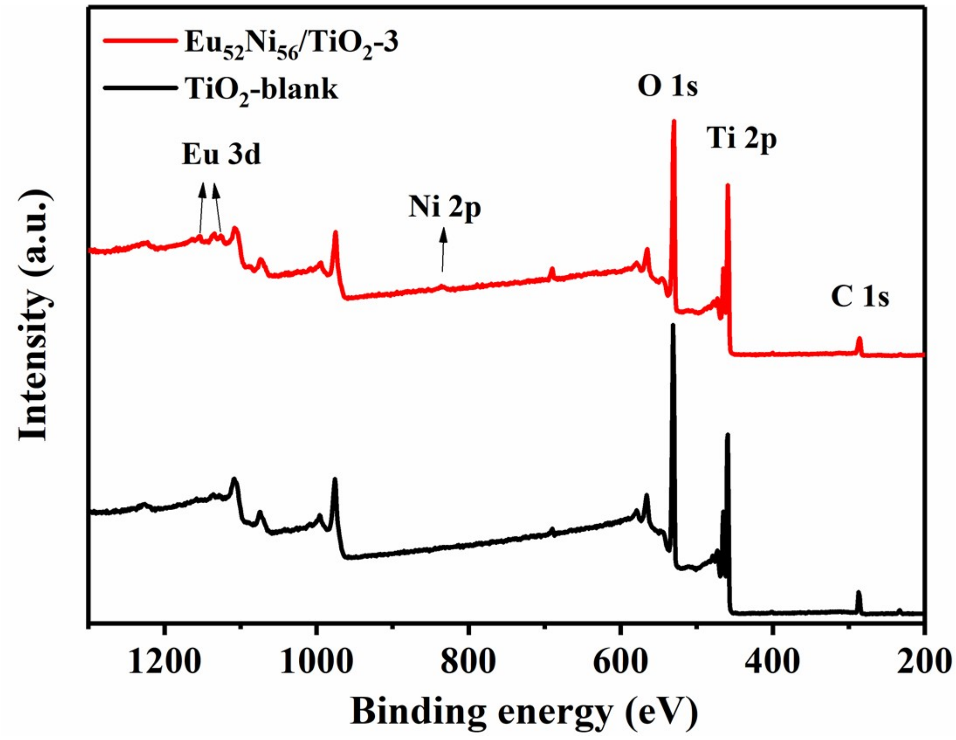

Figure S6. XPS full spectrum of TiO_2-blank and $Eu_{52}Ni_{56}/TiO_2$-3.

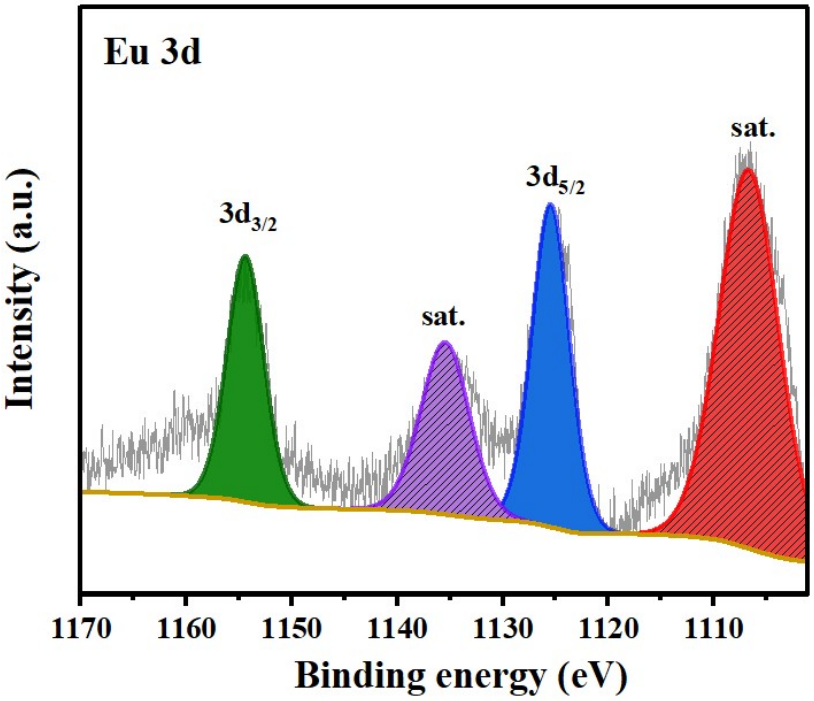

Figure S7. Eu 3d XPS profile of $Eu_{52}Ni_{56}/TiO_2$-3.

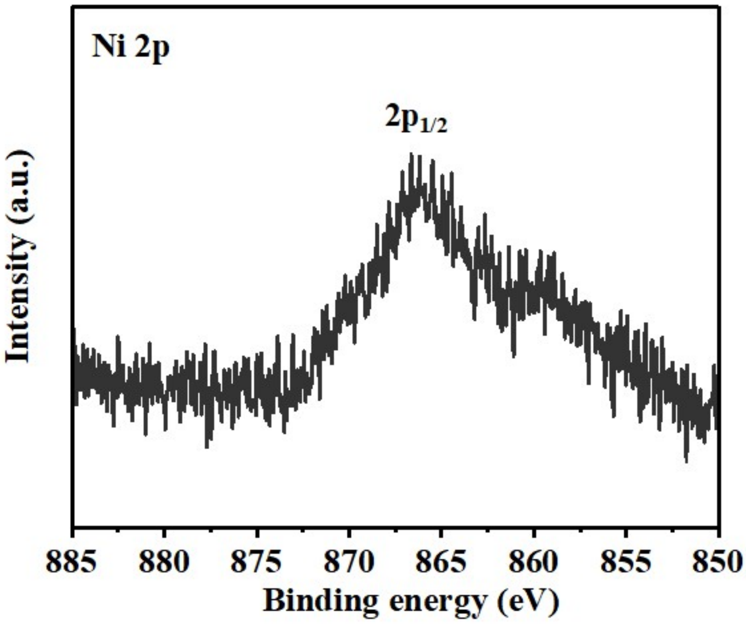

Figure S8. Ni 2p XPS profile of $Eu_{52}Ni_{56}/TiO_2$-3.

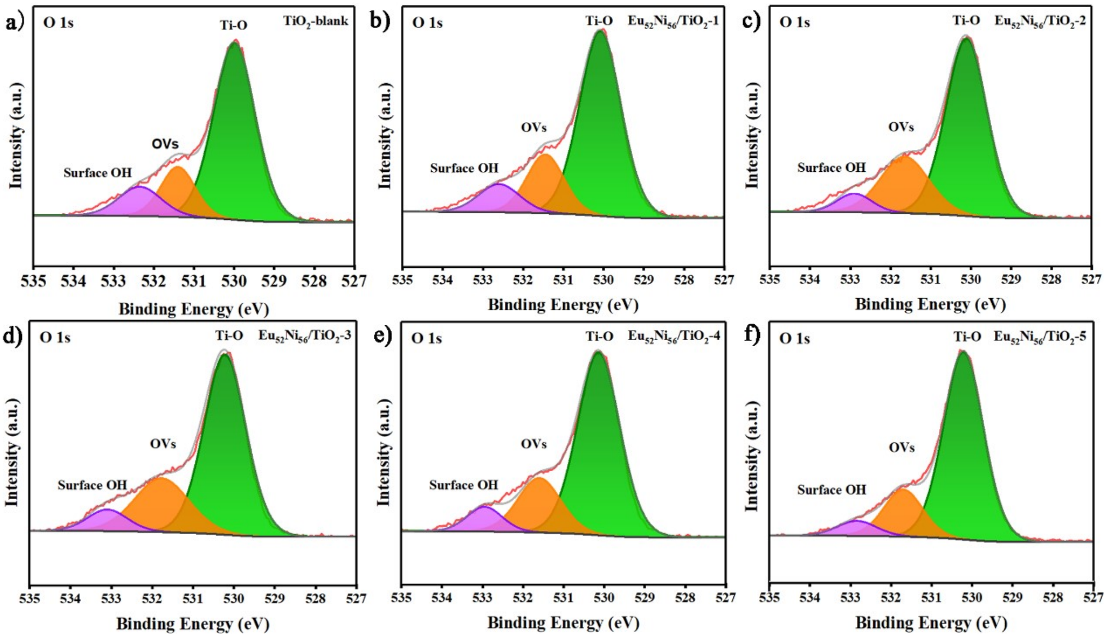

Figure S9. O 1s XPS profiles of TiO_2-blank and $Eu_{52}Ni_{56}/TiO_2$-1, 2, 3, 4, 5.

TiO_2-blank $Eu_{52}Ni_{56}/TiO_2$-1 $Eu_{52}Ni_{56}/TiO_2$-2 $Eu_{52}Ni_{56}/TiO_2$-3 $Eu_{52}Ni_{56}/TiO_2$-4 $Eu_{52}Ni_{56}/TiO_2$-5

Figure S10. Colors of TiO_2-blank and $Eu_{52}Ni_{56}/TiO_2$-1, 2, 3, 4, 5.

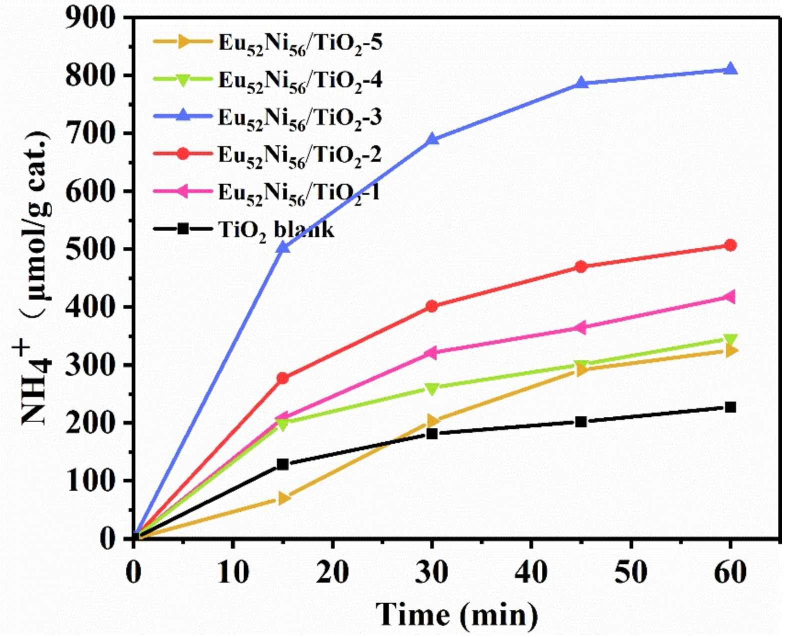

Figure S11. The catalytic efficiency of TiO_2-blank and $Eu_{52}Ni_{56}/TiO_2$-1, 2, 3, 4, 5.

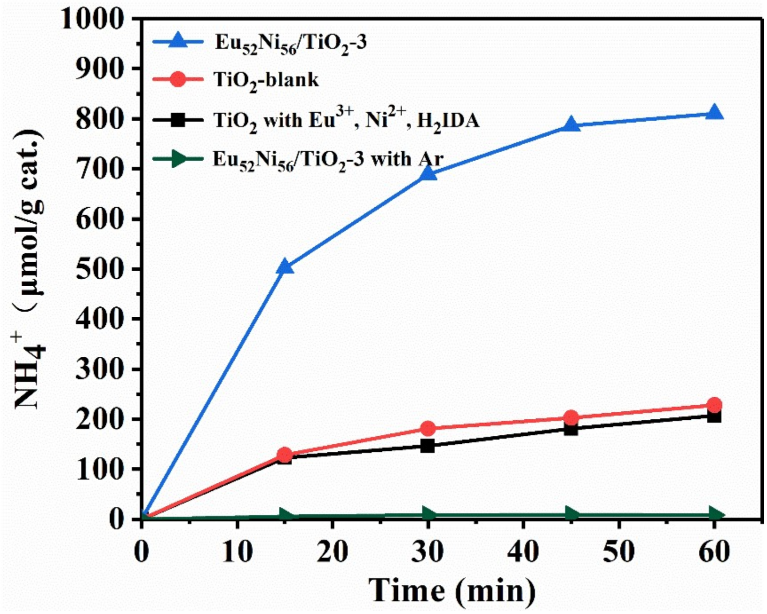

Figure S12. The comparative experiments for TiO_2-blank and $Eu_{52}Ni_{56}/TiO_2$-3.

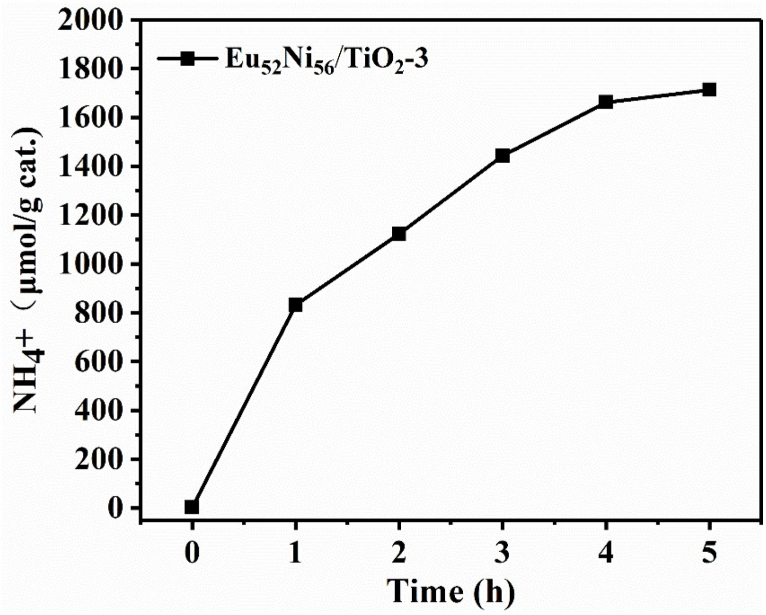

Figure S13. The yield of $Eu_{52}Ni_{56}/TiO_2$-3 was tested for 5 consecutive hours.

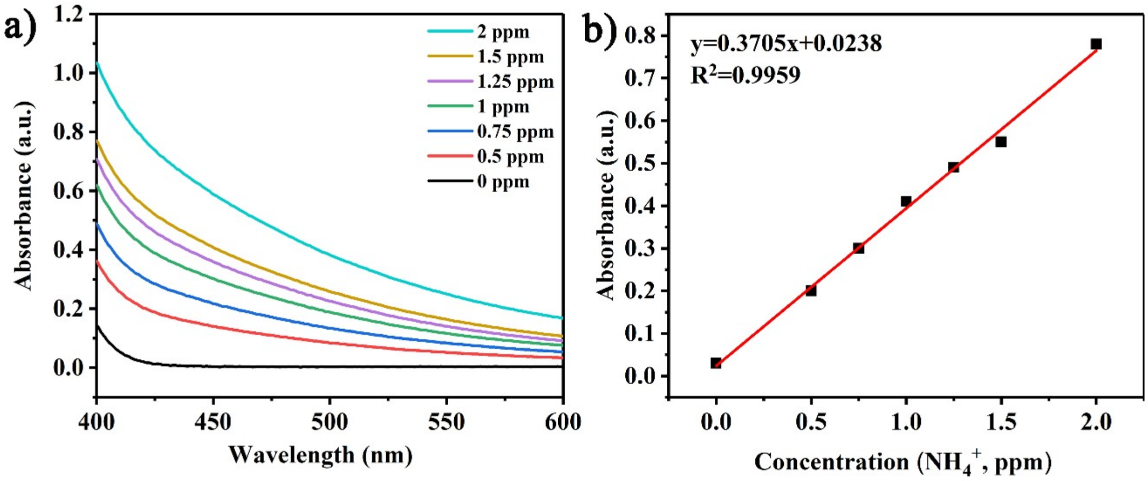

Figure S14. The UV absorption standard curve of NH_4^+ at wavelength of 420 nm which measured by Nessler reagent method.

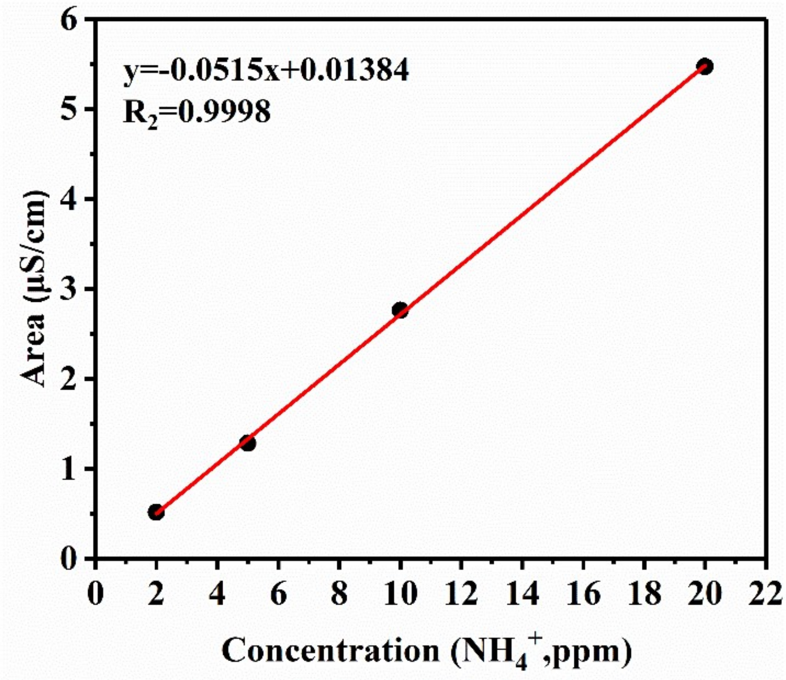

Figure S15. Standard curve of NH_4^+ with ion chromatography (ppm= mg/L)

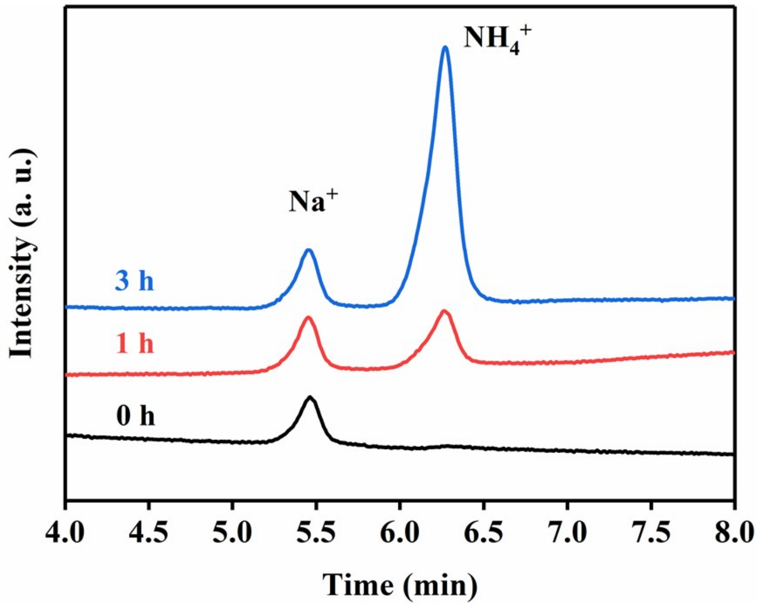

Figure S16. Ion chromatography (IC) data for NH_4^+generated from $Eu_{52}Ni_{56}/TiO_2$-3 under different time light exposure.

It should be noted that the quantification of NH_4^+ by Nessler's reagent method and ion chromatography yielded very similar results at this work. For example, the the yield of $Eu_{52}Ni_{56}/TiO_2$-3 tested by Nessler's reagent method and the yield tested by ion chromatography are 810 μmol·h^{-1}·g^{-1} and 779 μmol·h^{-1}·g^{-1}, respectively.

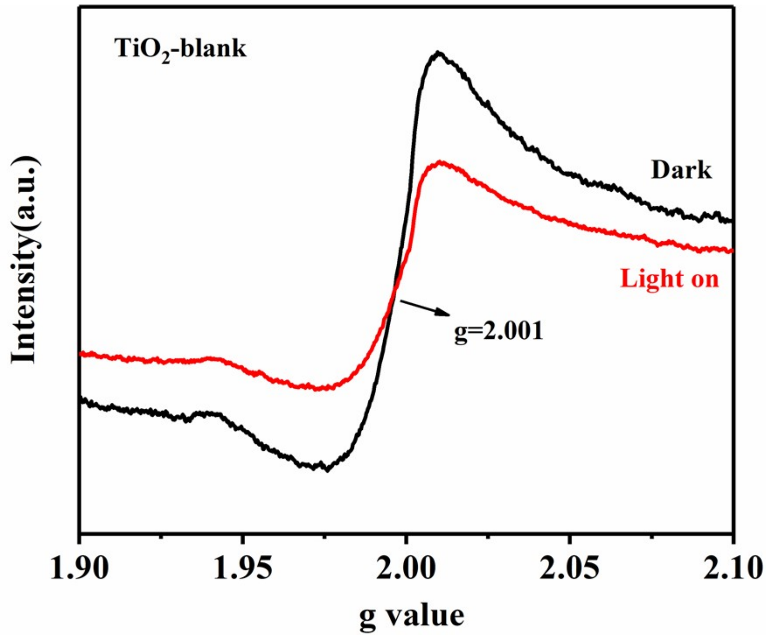

Figure S17. EPR spectra of TiO_2-blank under dark and light irradiation in 293K.

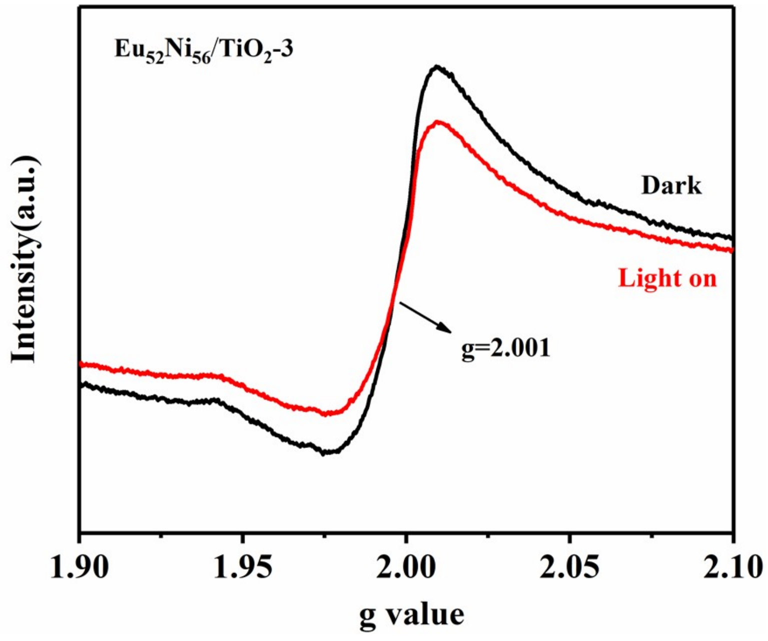

Figure S18. EPR spectra of $Eu_{52}Ni_{56}/TiO_2$-3 under dark and light irradiation in 293K.

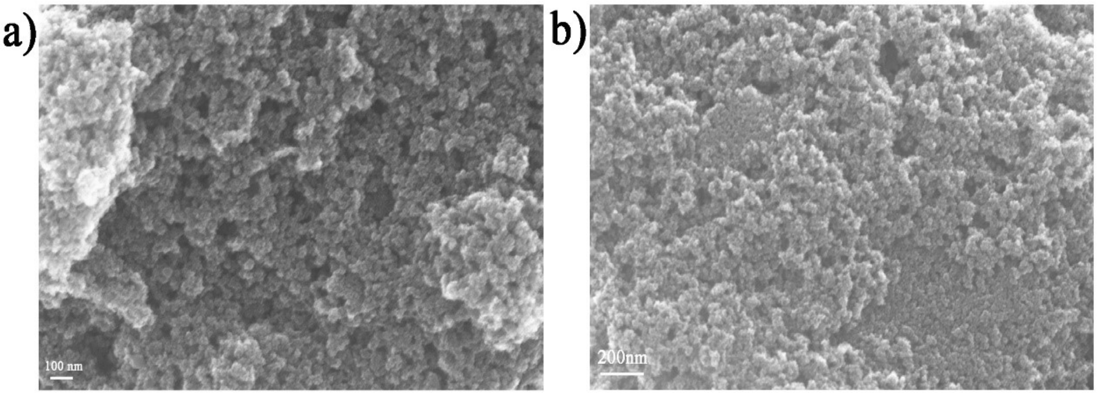

Figure S19. The comparison of the SEM morphology of catalyst $Eu_{52}Ni_{56}/TiO_2$-3 before (a) and after (b) catalysis.

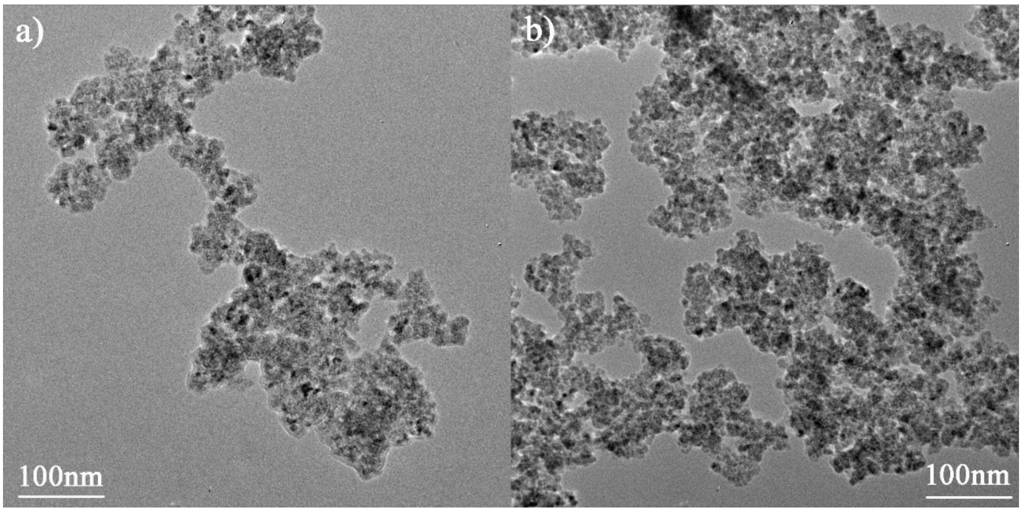

Figure S20. The comparison of the TEM morphology of catalyst $Eu_{52}Ni_{56}/TiO_2$-3 before (a) and after (b) catalysis.

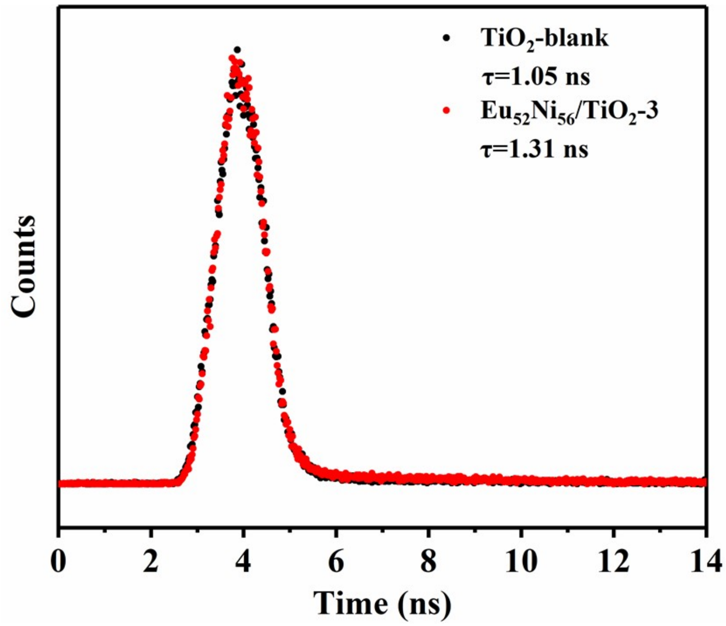

Figure S21. Time resolved fluorescence spectrum of TiO_2-blank and $Eu_{52}Ni_{56}/TiO_2$-3.

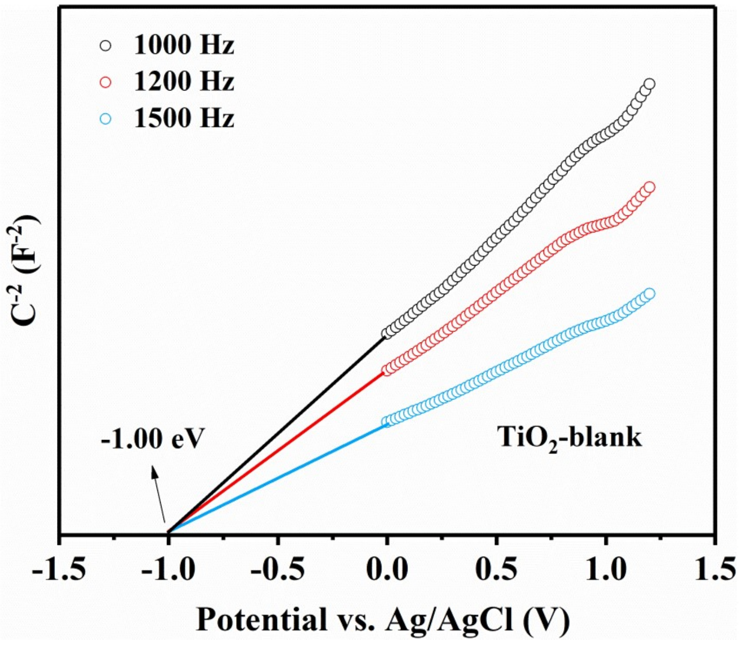

Figure S22. Mott–Schottky spots of TiO_2-blank in 0.2 M Na_2SO_4 (pH = 5.7) aqueous solution.

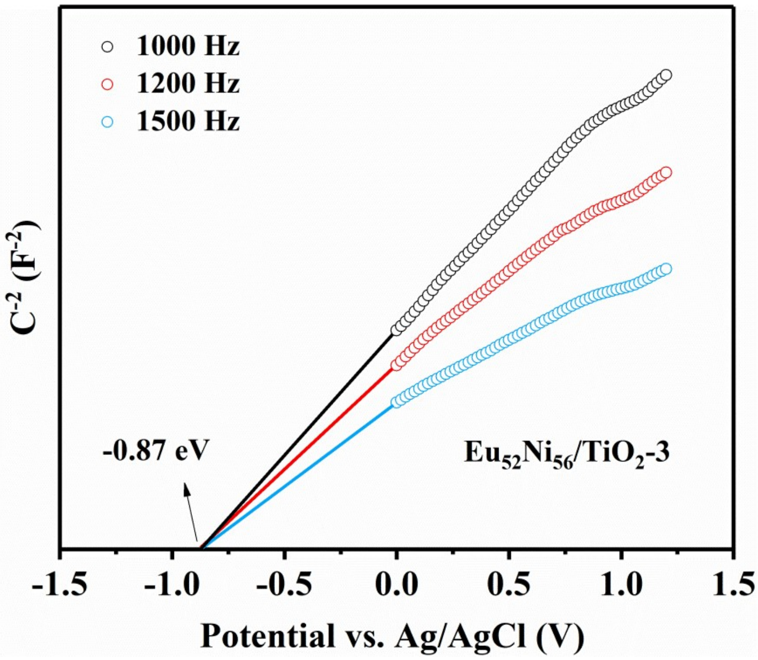

Figure S23. Mott–Schottky spots of Eu$_{52}$Ni$_{56}$/TiO$_2$-3 in 0.2 M Na$_2$SO$_4$ (pH = 5.7) aqueous solution.

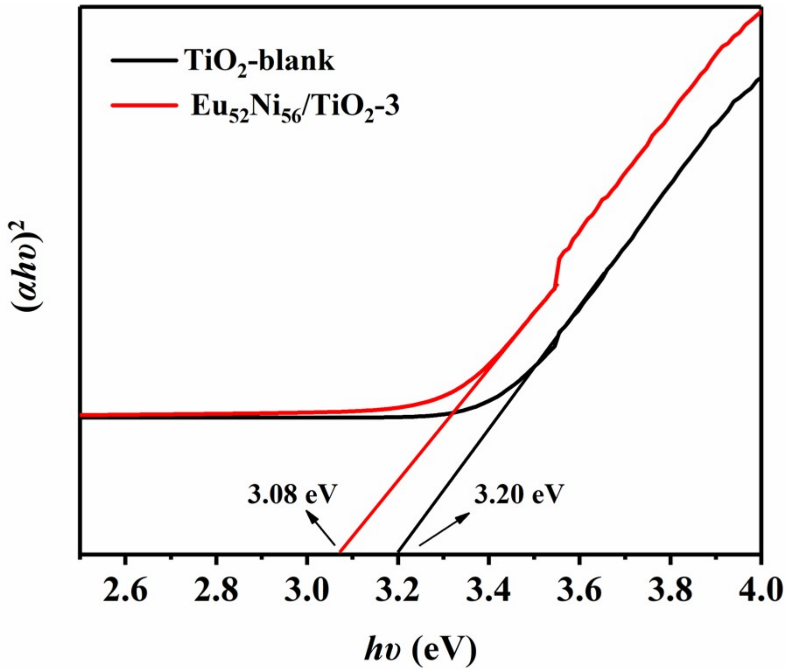

Figure S24. The band gap of Eu$_{52}$Ni$_{56}$/TiO$_2$-3 and TiO$_2$-blank.

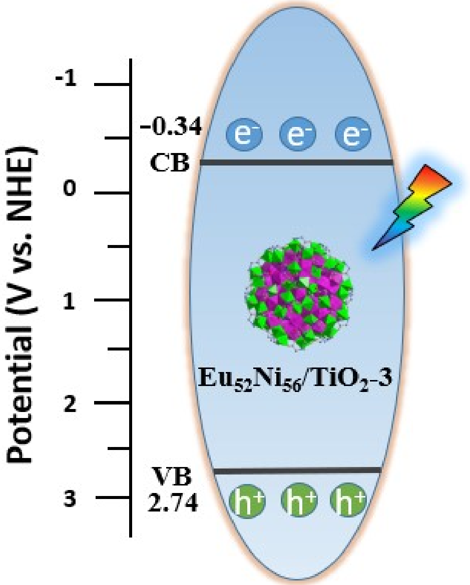

Figure S25. The location of VB and CB of $Eu_{52}Ni_{56}/TiO_2$-3.

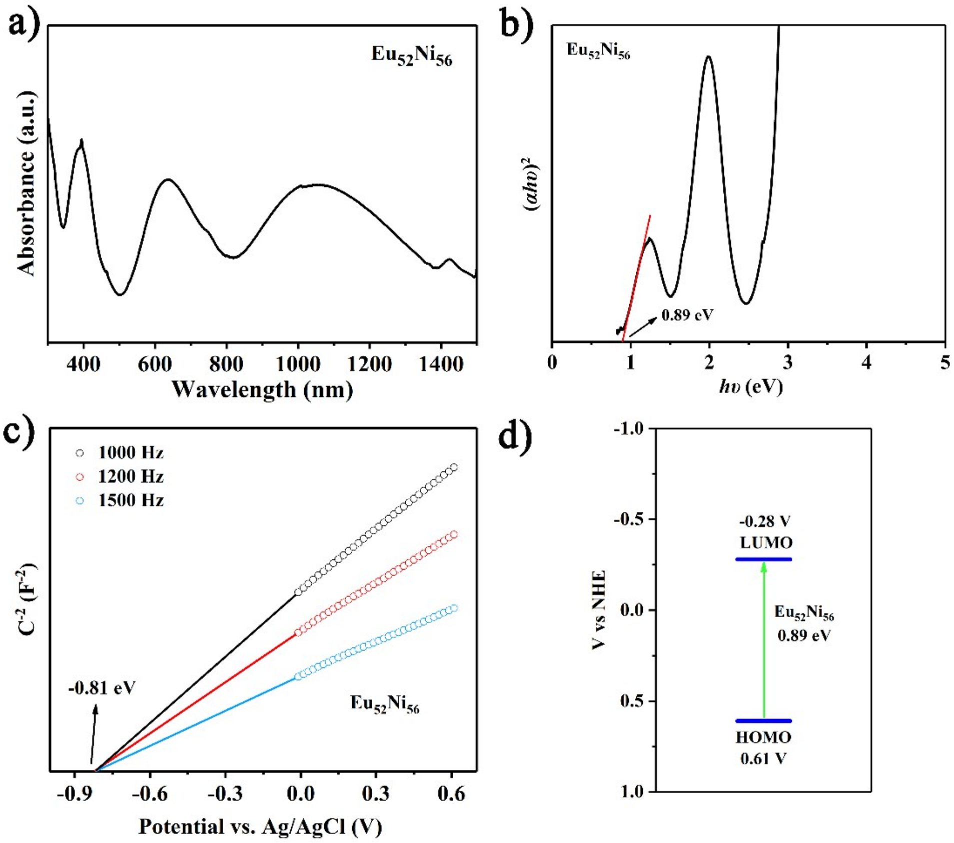

Figure S26. (a) The UV-vis diffuse reflectance spectra of $Eu_{52}Ni_{56}$. (b) The energy gap of $Eu_{52}Ni_{56}$. (c) The Mott–Schottky spots of $Eu_{52}Ni_{56}$ in 0.2 M Na_2SO_4 aqueous solution. (b) Energy band position of $Eu_{52}Ni_{56}$.

The UV-vis diffuse reflectance spectrum of the $Eu_{52}Ni_{56}$ shows the peak of d-d transition for octahedral Ni^{2+} at $\lambda = 1045$ nm, which are assigned to $^3A_{2g} \rightarrow {}^3T_{2g}$. The energy gap between $^3A_{2g}$ and $^3T_{2g}$ is consistent with the lowest energy gap between HOMO and LUMO energy level.[3] Therefore, the peak of ~1045 nm was used to calculate the energy gap of $Eu_{52}Ni_{56}$ with 0.89 eV.

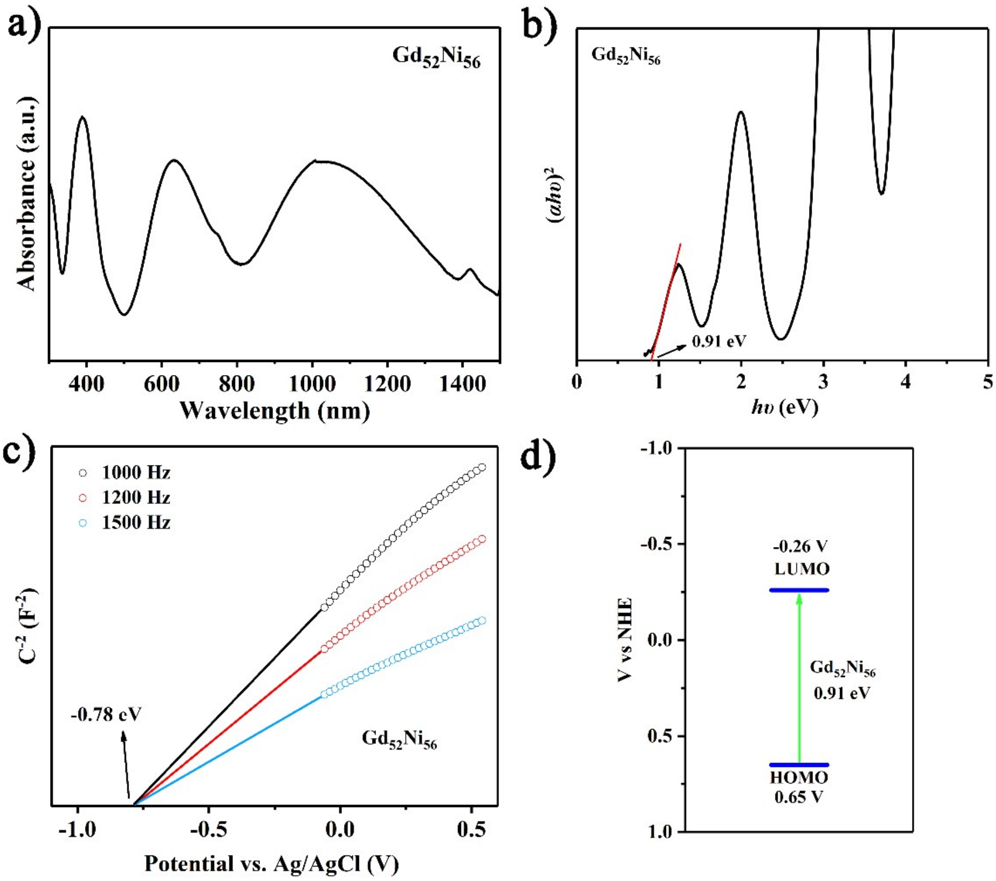

Figure S27. (a) The UV-vis diffuse reflectance spectra of $Gd_{52}Ni_{56}$. (b) The energy gap of $Gd_{52}Ni_{56}$. (c) The Mott–Schottky spots of $Gd_{52}Ni_{56}$ in 0.2 M Na_2SO_4 aqueous solution. (b) Energy band position of $Gd_{52}Ni_{56}$.

The peak of ~1045 nm was used to calculate the energy gap of $Gd_{52}Ni_{56}$ with 0.91 eV.

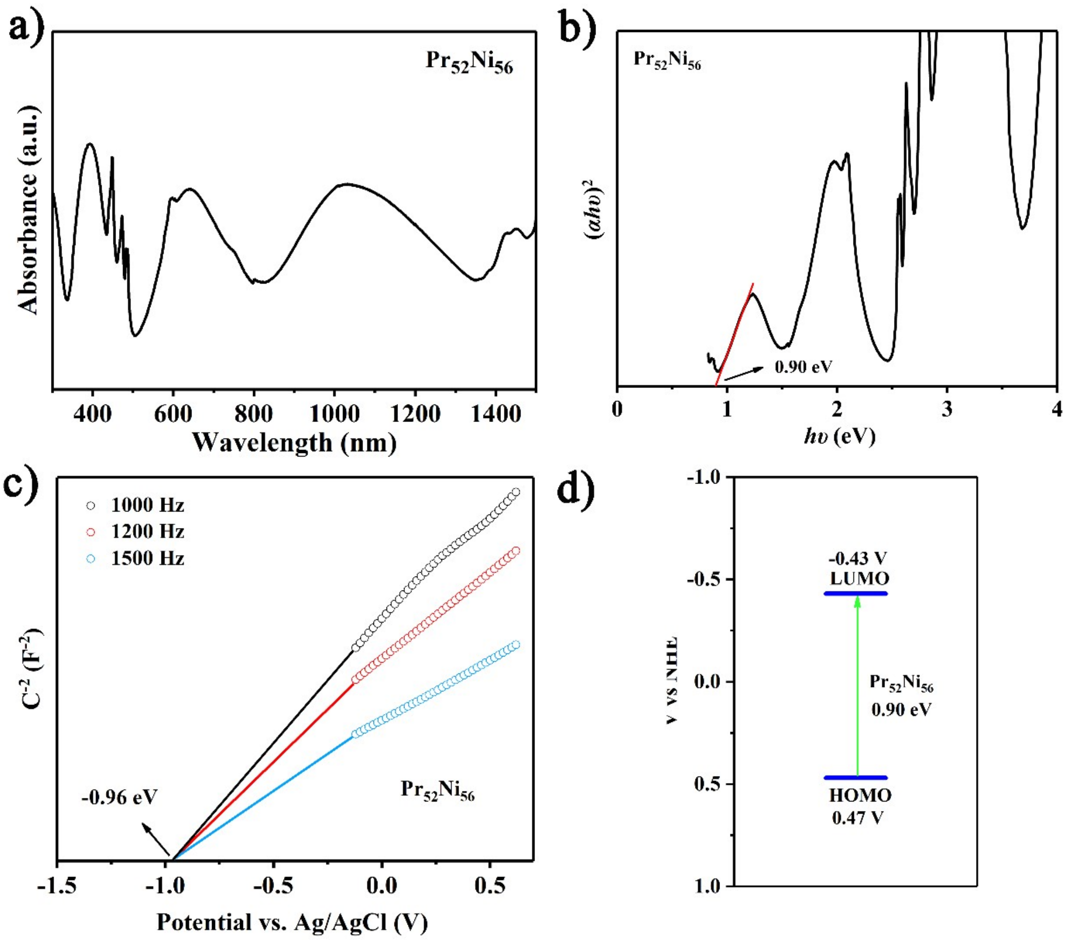

Figure S28. (a) The UV-vis diffuse reflectance spectra of $Pr_{52}Ni_{56}$. (b) The energy gap of $Pr_{52}Ni_{56}$. (c) The Mott–Schottky spots of $Pr_{52}Ni_{56}$ in 0.2 M Na_2SO_4 aqueous solution. (b) Energy band position of $Pr_{52}Ni_{56}$.

The peak of ~1045 nm was used to calculate the energy gap of $Pr_{52}Ni_{56}$ with 0.90 eV.

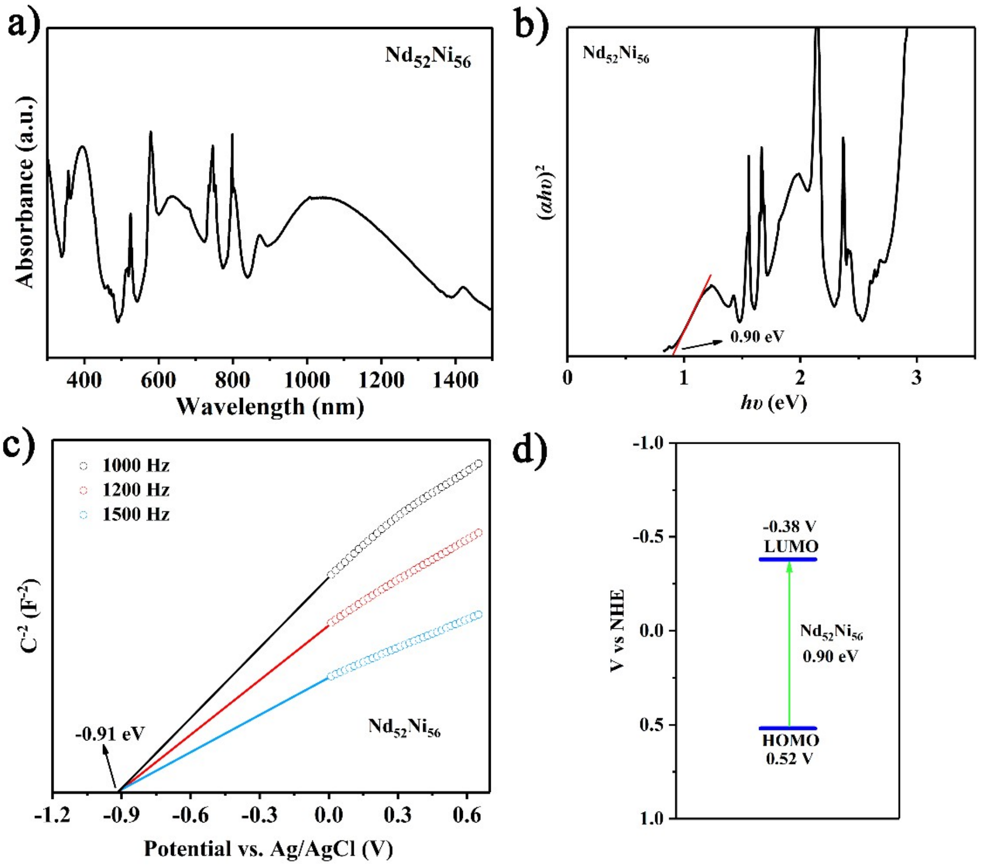

Figure S29. (a) The UV-vis diffuse reflectance spectra of $Nd_{52}Ni_{56}$. (b) The energy gap of $Nd_{52}Ni_{56}$. (c) The Mott–Schottky spots of $Nd_{52}Ni_{56}$ in 0.2 M Na_2SO_4 aqueous solution. (b) Energy band position of $Nd_{52}Ni_{56}$.

The peak of ~1045 nm was used to calculate the energy gap of $Nd_{52}Ni_{56}$ with 0.90 eV.

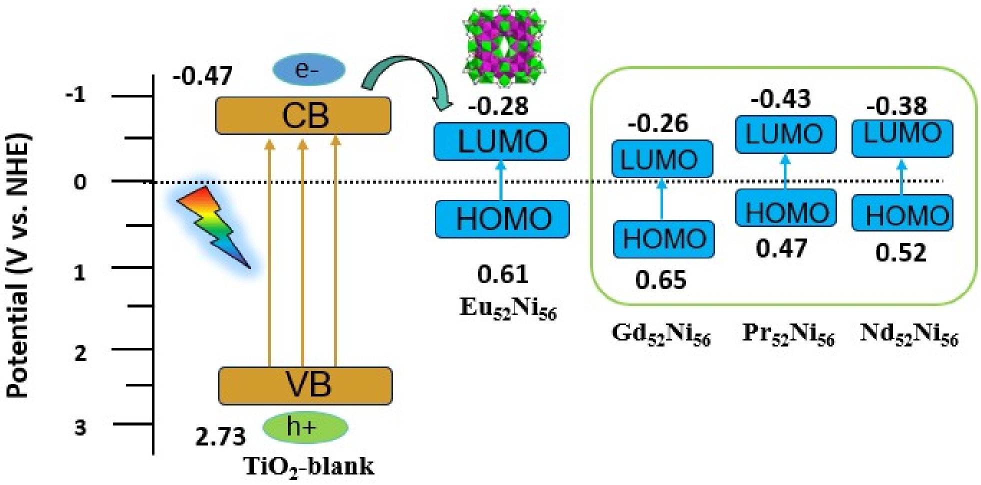

Figure S30. Charge separation and transfer between TiO_2-blank and $Ln_{52}Ni_{56}$.

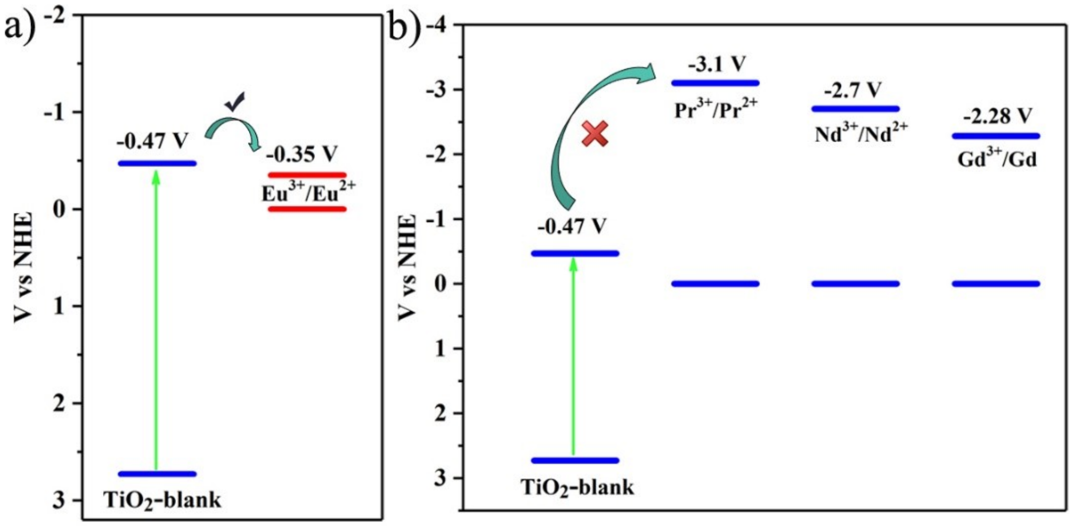

Figure S31. The energy levels of TiO_2-blank, Eu^{3+}/Eu^{2+}, Pr^{3+}/Pr^{2+}, Nd^{3+}/Nd^{2+} and Gd^{3+}/Gd reduction potentials.

Table S1. Integration of the XPS O 1s profiles area of TiO_2-blank and $Eu_{52}Ni_{56}/TiO_2$-1, 2, 3, 4, 5.

Species Samples	OH	OVs	Ti-O	Proportion of OVs
TiO_2-blank	21537.75	34040.84	127072.31	18.6%
TiO_2-$Eu_{52}Ni_{56}$-1	17113.53	32384.46	113258.09	19.9%
TiO_2-$Eu_{52}Ni_{56}$-2	9576.67	40427.17	124145.96	23.2%
TiO_2-$Eu_{52}Ni_{56}$-3	12328.95	41733.08	107737.5	25.8%
TiO_2-$Eu_{52}Ni_{56}$-4	13563.46	36714.21	141772.49	19.1%
TiO_2-$Eu_{52}Ni_{56}$-5	9831.8	35223.19	146895.08	18.4%

References

[1] R. Chen, Z. H. Yan, X. J. Kong, L. S. Long, L. S. Zheng, *Angew. Chem. Int. Ed.* **2018**, *57*, 16796-16800.

[2] Y. Zhao, R. Shi, X. Bian, C. Zhou, Y. Zhao, S. Zhang, F. Wu, G. I. N. Waterhouse, L. Z. Wu, C. H. Tung, T. R. Zhang, *Adv. Sci.* **2019**, *6(8)*, 1802109.

[3] L. E. Orgel, *J. Chem. Phys.* **1955**, *23*, 1004-1014.